Check for updates

Machine learning and chemometrics for electrochemical sensors: moving forward to the future of analytical chemistry

Pumidech Puthongkham, [ID] *[a,b,c] Supacha Wirojsaengthong[a] and Akkapol Suea-Ngam[d]

Electrochemical sensors and biosensors have been successfully used in a wide range of applications, but systematic optimization and nonlinear relationships have been compromised for electrode fabrication and data analysis. Machine learning and experimental designs are chemometric tools that have been proved to be useful in method development and data analysis. This minireview summarizes recent applications of machine learning and experimental designs in electroanalytical chemistry. First, experimental designs, *e.g.*, full factorial, central composite, and Box–Behnken are discussed as systematic approaches to optimize electrode fabrication to consider the effects from individual variables and their interactions. Then, the principles of machine learning algorithms, including linear and logistic regressions, neural network, and support vector machine, are introduced. These machine learning models have been implemented to extract complex relationships between chemical structures and their electrochemical properties and to analyze complicated electrochemical data to improve calibration and analyte classification, such as in electronic tongues. Lastly, the future of machine learning and experimental designs in electrochemical sensors is outlined. These chemometric strategies will accelerate the development and enhance the performance of electrochemical devices for point-of-care diagnostics and commercialization.

1. Introduction

Electrochemical sensors have been widely developed and settled into a period of sustained growth with diverse applications across environmental, food, and biomedical fields.[1,2] The optimization of electrode materials and detection conditions is essential to maximize sensor performance. However, most studies typically optimize one variable at a time,[3] which is straightforward but problematic, especially if two or more variables interact with each other.[4] The conditions determined to prepare and operate the sensor might not be the true optimum, preventing the ultimate applications of the electrochemical sensors in the field or point-of-care diagnostics. A chemometric tool named experimental design or design of experiment (DoE) has been invented for systematically and

statistically valid parameter optimization.[4] However, electrochemists may still be reluctant to utilize this advantageous method to fabricate and optimize their sensors.

Recently, machine learning (ML) has become a popular method to analyze complex relationships in experimental data.[5] It has been found to be a crucial tool to predict quantitative structure–activity relationship of drugs and biologically active molecules effectively.[6] Deep learning, one of the most popular ML algorithms, has the potential to analyze data from continuous sensing for anomaly detection, instrumental failure,[7] or Internet of Things.[8] For analytical chemistry, there are emerging opportunities for ML,[9] such as integration in the lab-on-a-chip device to quantify and classify molecules and biological moieties.[10,11] Furthermore, ML has been utilized in several electrochemical applications. The electrochemical impedance spectra (EIS) of Li-ion batteries were analyzed by ML to predict their remaining battery capacity.[12] ML was also combined with density functional theory (DFT) calculation to predict the energy levels and redox potentials of organic battery electrodes.[13] For organic electrosynthesis, the cyclic voltammogram (CV) of organic compounds were correlated with the reaction yield to optimize a synthetic route.[14] Text mining and natural language processing were also implemented to extract the experimental data from published articles to find

[a]Department of Chemistry, Faculty of Science, Chulalongkorn University, Bangkok 10330, Thailand. E-mail: Pumidech.P@chula.ac.th
[b]Electrochemistry and Optical Spectroscopy Center of Excellence (EOSCE), Chulalongkorn University, Bangkok 10330, Thailand
[c]Center of Excellence in Responsive Wearable Materials, Chulalongkorn University, Bangkok 10330, Thailand
[d]Department of Materials, Department of Bioengineering, and Institute of Biomedical Engineering, Imperial College London, London, SW7 2AZ, UK

the best battery and electrolyte composition.[15] Nevertheless, ML applications in electroanalytical chemistry are still limited,[9] since the data are complicated and not always straightforward to build an expansive database.

This article summarizes the recent applications of DoE and ML in developing electrochemical sensors and analyzing their data. The basic concepts and the roles of common DoE in planning and optimizing parameters in electrochemical sensors and detection will be first discussed. Then, the brief fundamentals of ML algorithms and their applications to reveal the hidden knowledge in electrochemistry and to interpret and extract qualitative and quantitative information from electrochemical data will be examined. Finally, the future of DoE and ML in analytical electrochemistry will be forecasted. Indeed, DoE and ML are beneficial for all analytical techniques, but electrochemistry research is currently underutilizing them. Using DoE for optimizing electrochemical sensors and ML in data analysis will maximize their potential for complicated sample analysis and point-of-care applications. We hope that this review will encourage the readers in electrochemical science to appreciate the potential benefits of these emerging methods and to apply them in future research. Implementing DoE and ML for sensor fabrication and data analysis will improve their performance for real samples and will aid the digitization of chemical experiments[16] to meet the future demand.

2. Experimental design for optimizing electrochemical sensors

2.1. Common experimental designs

Optimization of the sensor fabrication and detection parameters is the key step to maximize the analytical performance of electrochemical sensors. Traditionally, one-factor-at-a-time (OFAT) is the experimental design that has been leveraged and mounted as the standard optimization in analytical chemistry by varying one parameter at a time while fixing others.[17] This dominating design assumes that each factor is not influenced by others, thus the optimum value of each factor can be determined separately then combined together later. This approach is simple, but it has many obvious drawbacks—OFAT requires a lot of experiments.[3] For example, investigating an experiment with parameters including five pH values and five concentrations with five replicates for each condition requires 125 runs. Performing these many experiments exploits unnecessary time and cost, generates unnecessary waste, and is unsustainable. Another limitation is that OFAT does not consider the cooperative effect from the interaction between factors, leading to the lack of promise for obtaining the true optimal.[17] These problems are critical for developing biosensors with complicated mechanisms and instrumentation, especially for point-of-care diagnostics in resource-limited areas.

Plackett–Burman design. To address problems from OFAT design, many DoEs have been proposed to empower the optimization with a smaller number of experiments but gaining more informative results. One of the earliest and simplest DoEs is Plackett–Burman Design (PBD), which utilizes upper (+) and lower (−) levels of each factor and requires only $N + 1$ experiments to screen N variables.[17] Fig. 1A illustrates that only four experiments are required for three factors. That being said, PBD is frequently used to screen for the significant parameters for further optimization by other designs.[17] For instance, Filgueiras and coworkers used PBD to determine the significant parameters among seven parameters in extracting microplastic from marine sediments.[18] PBD required only eight experiments and revealed that sediment mass and agita-

From left to right: Akkapol Suea-Ngam, Supacha Wirojsaengthong, and Pumidech Puthongkham

Pumidech Puthongkham is a faculty member at the Department of Chemistry, Faculty of Science, Chulalongkorn University. In 2020, he earned his Ph.D. in analytical chemistry from the University of Virginia, where he worked with Prof. B. Jill Venton. He was a recipient of the Anandamahidol Foundation Scholarship. His research interests focus on the development of high-performance electrochemical sensors, electrochemistry at carbon electrodes, and machine learning and complex data analysis for analytical chemistry.

Supacha Wirojsaengthong earned her Ph.D. in analytical chemistry from the Department of Chemistry at Chulalongkorn University in 2021 under the supervision of Assoc. Prof. Wanlapa Aeungmaitrepirom. She earned the Development and Promotion of Science and Technology Talent project (DPST) scholarship for her bachelor and doctoral studies supported by Thailand. Her research interests include developing new analytical tools using an ion selective electrode and a bulk optode system.

Akkapol Suea-Ngam is a recipient of SNSF Early.Postdoc Mobility (2021–2022) as a postdoctoral associate at the Stevens Group, Imperial College, UK. He completed his Doctor of Science (Dr Sc.) from deMello Group, ETH Zürich, Switzerland, supported by the Swiss Government Excellence Scholarship. His research interest includes experimental design, microfluidics, electrochemical and optical approaches for point-of-care diagnostics, and nanomaterial applications.
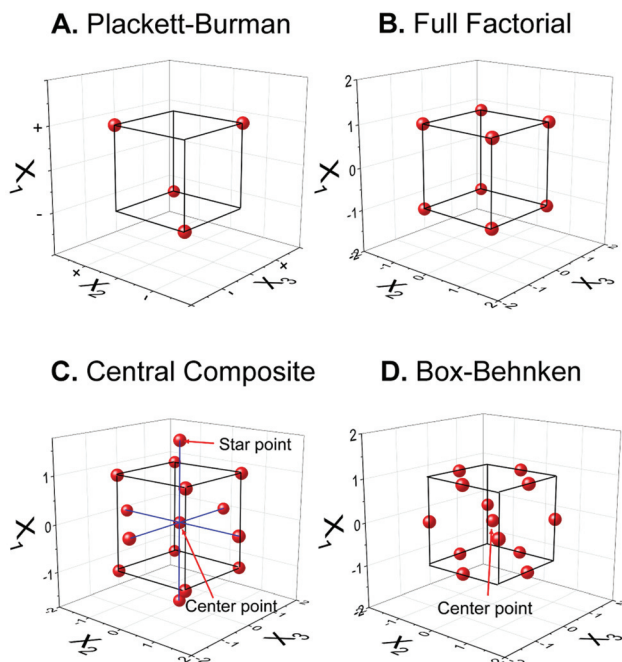
A. Plackett-Burman

B. Full Factorial

C. Central Composite

D. Box-Behnken

Fig. 1 Two-level experimental designs illustrated for three parameters, X_1, X_2, and X_3. (A) Plackett–Burman design, (B) full factorial design, (C) central composite design, and (D) Box–Behnken design.

tion time are the most significant variables to be further optimized. This approach therefore efficiently saves cost and time from performing many experiments. However, PBD is effective for only a linear relationship between response and factors.[3]

Factorial designs. Another common DoE is Full Factorial Design (FFD), which investigates the variable main effects and interaction effects on the response.[17] FFD designates L levels for each variable, so it needs L^N experiments to investigate N variables. Fig. 1B visualizes eight experiments for two-level, three-factor factorial designs as the box vertices. Then, the response is modeled by considering the interaction between factors. Considering three variables X_1, X_2 and X_3, the response Y includes three main effects, three two-factor interactions, and one three-factor interaction as ordered in (1).

$$Y = \beta_0 + \beta_1 X_1 + \beta_2 X_2 + \beta_3 X_3 + \beta_{12} X_1 X_2 \\ + \beta_{13} X_1 X_3 + \beta_{23} X_2 X_3 + \beta_{123} X_1 X_2 X_3 \tag{1}$$

The magnitude of each β coefficient illustrates the impact or significance of each factor and interaction. Kechagias *et al.* reported the three-level FFD to model the machinability prediction in turning of a Ti-6Al-4V alloy, which has three parameters, thus 27 runs were performed.[19] Nevertheless, although the FFD can solve the OFAT lacking of interaction consideration, the number of FFD runs is still large. One way to reduce the number of experiments is to use Fractional Factorial Design (FrFD), which keeps only half or quarter of the points from FFD to eliminate its redundancy between the runs.[17] Nevertheless, FFD does not consider higher-order terms such

as quadratic behavior, so it may prevent some undesired phenomena such as nonlinear noise to be accounted for.

Central composite design. Central Composite Design (CCD) has been leveraged and developed from FFD by adding the runs at the "center" and "star" points in the model, as illustrated in Fig. 1C.[17,20] Adding these points allows the quadratic terms (such as $\beta_{11} X_1^2$, $\beta_{22} X_2^2$, and $\beta_{33} X_3^2$) to be investigated in addition to the linear individual and interaction effects. By adding C points at the box center, the number of experiments is $2^N + 2N + C$, for two-level CCD, which is considerably less than that of OFAT. However, CCD is appropriate for two to five variables, since the differences are not considerable for more variables. For example, concentrations of the ion exchanger and ionophore were optimized by 13 experiments from two-level CCD to fabricate a colorimetric sensor for thiocyanate detection.[21] CCD was also applied to optimize the current density, electrolysis time, flow rate, and anode material for the electrochemical removal of carbamazepine using Ti composite electrodes.[22]

Box–Behnken design. Box–Behnken Design (BBD) is useful when the extreme, higher-order effect such as the quadratic term can be neglected, requiring only three levels for each parameter while CCD requires five. Thus, the number of BBD experiments is $2N(N - 1)C$. Accordingly, to reduce the number of experiments from that of CCD, BBD eliminates the star points and replaces them with points on the box edges (Fig. 1D).[17] This design allows avoiding experiments under extreme conditions, which do not contain an embedded FFD or FrFD. Ahmadi and Ghanbari utilized BBD to optimize the photoelectro-persulfate method to investigate the pH, persulfate concentration, current density, and electrolysis time to decrease the chemical oxygen demand in greywater.[23]

2.2. Method optimization from the response surface methodology

The next step after performing experiments according to the chosen DoE is to determine the optimum point. Response surface methodology (RSM) visualizes the relationship between a pair of variables by plotting the response surface.[24] With the surface, more understanding of the whole experimental system is achieved and leads to improved optimization.[24] For example, the effect of pH on the measurement of glucosamine using a gold nanoparticle (AuNP)/polyaniline-modified electrode was illustrated as a stack of response surfaces (Fig. 2A), which clearly displayed that lower pH increases the signal.[25] From it, a contour plot of the chosen pH can be constructed from the surface to find the optimum amount of AuNPs and polyaniline (Fig. 2B).

Another advantage of RSM is to evaluate the effect on the response if the variables are shifted, as sometimes the mathematically derived optimal condition is not convenient to perform. If the slope of the surface is not too large, then slightly shifting the value from the optimal may ease the experimental setting while preserving the nearly optimized condition. Alternatively, a surface contour plot of the electrochemical signal with gradual color mapping can visualize the
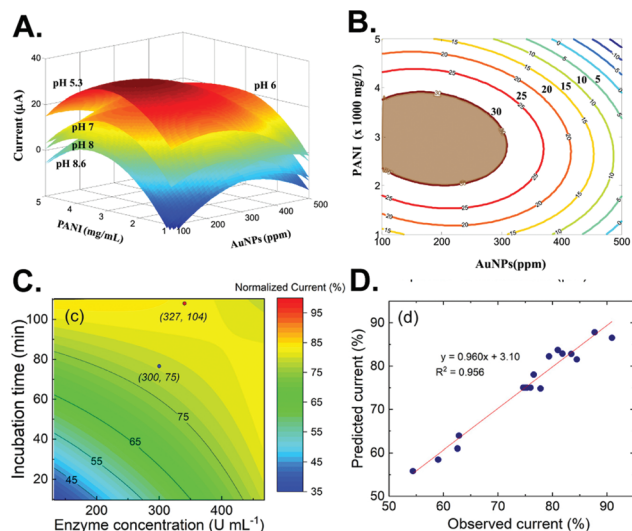
Fig. 2 Example of RSM for electrochemical sensor optimization. (A) Surfaces from different pH combined with the effect of gold nanoparticles and polyaniline on glucosamine detection. (B) A contour plot of the chosen pH from (A). Reprinted from ref. 25 with permission from Elsevier. (C) A surface contour plot of the enzyme concentration and incubation time for enzymatic biosensor optimization. (D) Correlation between the observed and predicted response. Adapted with permission from ref. 26. Copyright 2019 American Chemical Society.

2.3. Experimental design for optimizing electrochemical sensors and waveforms

DoE with RSM has gained popularity for electrochemical sensor optimization with more than one independent variable. Ören Varol *et al.* utilized FFD to perform 17 runs to optimize the amount of two modifiers, pH, and scan rate for graphene/azobenzene-perylene diimide derivative-modified carbon paste electrode for dopamine detection.[28] RSMs between each pair of variables were plotted to determine the optimum point, and the optimized sensor has a detection limit (LoD) of 0.26 μM. Brahma *et al.* used BBD to optimize functionalized multi-walled carbon nanotubes (fMWCNT), ethylenedioxythiophene (EDOT), and *o*-phenylenediamine (*o*-PD) to modified a glassy carbon electrode for *p*-chlorometaxylenol detection.[29] The chosen DoE and RSM allows the optimization of fMWCNT electrodeposition and EDOT and *o*-PD electropolymerization to maximize the response from the analyte from their electrocatalytic properties without the diminishing effect from the polymer thickness. Hendawy *et al.* also utilized FrFD to screen the significant factors in the fabrication of the graphene oxide/MWCNT/carbon paste electrode and the square wave voltammetry (SWV) waveform for the simultaneous voltammetric

determination of paracetamol, guaifenesin, and ascorbic acid.[30]

Multiple DoEs can be subsequently implemented to screen important variables and to optimize the electrode preparation. A non-enzymatic lactose sensor based on a molecular imprinted polymer on a graphite paper electrode was optimized.[31] PBD was utilized to screen seven factors including lactose template concentration, pyrrole monomer concentration, electropolymerization cycle, lactose extraction, electropolymerization pH, lactose rebinding time, and rebinding pH. Only three of these factors were significant and subsequently optimized by CCD, improving the LoD of the sensor to 0.88 nM. For more complicated biosensors, Rizi *et al.* prepared an electrochemical DNA biosensor to detect *Mycobacterium tuberculosis* based on complementary target hybridization.[32] Again, 11 variables from the electrode fabrication (probe concentration and immobilization time) and detection (such as electrochemical parameters, pH, and temperature) were screened by PBD. CCD was subsequently optimized for the most significant variables: buffer molarity, probe concentration, and differential pulse voltammetry (DPV) scan rate. The optimized biosensor had a LOD of 0.141 nM with a wide linear range. These studies showed that performing thorough optimization by CCD with only significant parameters screened by PBD is a useful strategy.

3. Machine learning for developing electrochemical sensors and analyzing electrochemical data

3.1. Classification of electrochemical data

Electrochemical techniques are diverse and thus provide data with different dimensionality or orders (Fig. 3), which are compatible with different ML algorithms.[33] Zero-order (or zero-dimensional) data are obtained from an electrochemical measurement that gives a single value (Fig. 3A). For example, a pH meter or a potentiometric ion-selective electrode gives a single pH or p-ion value from each sample or measurement.[34] Zero-dimensional data can be treated by univariate analysis, such as simple linear regression between ion-selective electrode potential and p-ion.
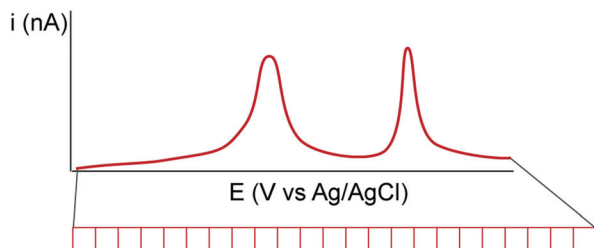
First-order (or one-dimensional) data are given from a technique which measures the value of a dependent variable from a varied independent variable and can be treated as a vector (Fig. 3B). Many electrochemical experiments fall into this category, such as chronoamperometry (current from a single applied potential *vs.* time) and voltammetry (current *vs.* applied potential). One-dimensional data can be treated by multivariate data analysis if the whole vector of data is utilized. For example, DPV of a mixture can be analyzed by principal component analysis (PCA) and regression (PCR) to identify the compounds and their concentrations.[35] However, from the same technique, a single data point can be chosen to be analyzed, *e.g.*, current at a selected potential, to reduce the

The difference between the mathematically derived optimum point (red) and the chosen point (blue), as implemented in enzymatic sensor optimization (Fig. 2C).[26] Subsequently, the predicted and observed experimental results from using such different conditions can be statistically compared to evaluate the model (Fig. 2D).[25–27]

A. Zero-order data

sample 1   sample 2

B. First-order data

i (nA)

E (V vs Ag/AgCl)

C. Second-order data
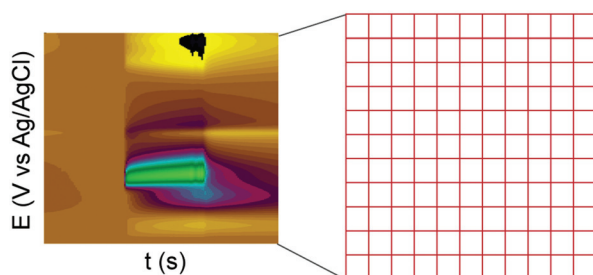
E (V vs Ag/AgCl)

t (s)

Fig. 3 Classification of electrochemical data by their order. (A) Zero-order electrochemical data such as single pH measurement give a single data point. (B) First-order data such as those from DPV give a vector of current *vs.* potential. (C) Second-order data such as data from FSCV give a matrix of current *vs.* potential *vs.* time.

problem to the zero-order, and the more simple univariate analysis can be applied.

Second-order (or two-dimensional) data are obtained from a technique with two independent variables varied together, so the data can be plotted as a matrix (Fig. 3C). Spectroelectrochemistry is one technique that gives second-order data from one dependent variable (absorbance) and two independent variables (wavelength and applied potential).[36] Fast-scan cyclic voltammetry (FSCV), a dominating electrochemical technique for *in vivo* detection of neurotransmitters, also gives two-dimensional data of the current from the varied potential (triangular waveform) and time.[37] Treatment of second-order electrochemical data is complicated because of the extra dimension. Reducing the data to first-order by PCA or manually choosing a single applied potential to analyze the data for visualization is possible, but huge amounts of information is eliminated by this approach. One feasible strategy to deal with second-order data is to plot the data matrix as an image, and the problem can be reduced to image recognition, with numerous ML and processing algorithms available.[38,39] Higher-order data are also possible for techniques which vary more than two variables simultaneously.

3.2. Common machine learning algorithms

ML is an automated method for data analysis to make a decision without any explicit instruction. The algorithms "learn" the decision rule from the given data, which is called "training set". One distinct property of ML is that its performance is improved when it is trained with more data, therefore a large set of experiments must be performed to build the training set to maximize the performance of ML.[5] In general, ML problems can be classified into supervised and unsupervised learning.[9] Supervised learning analyzes the relationship between the independent variables ("features"), and the dependent variables ("label"), and it uses the discovered relationship to predict the label of new data from their features. Supervised learning can be categorized into regression and classification.[40] The problem of quantifying the unknown concentration is regression, while identifying the chemical species is classification. In contrast, unsupervised learning deals with the unlabeled data to find the inherent structure to cluster the data into groups. To the best of our knowledge, unsupervised ML has not been utilized for electrochemical sensors, but it was utilized to group unknown biological tissues from their mass spectra for omics applications to discover the similarity or network between their biological activities.[41]

There are many ML algorithms or models. The following list includes only supervised learning models and is not exhaustive. Further mathematical details on the algorithm, cost function, and decision rule updating can be found elsewhere.[9,40,42]

Linear regression. Linear regression (Fig. 4A) is the most common procedure in quantitative chemical analysis to determine the quantitative label from the features, such as to estimate the concentration from the voltammetric peak current.[43] Simple univariate linear regression is the special case to find the linear function between one feature x and one label y. That is, to find the best β_0, β_1 coefficients that give the best function (2).

$$y = \beta_0 + \beta_1 x \qquad (2)$$

The most familiar method to find the best coefficients is the least squares method, which is to minimize the average of the squared difference between the predicted and the true label.[40]

Multiple linear regression deals with more than one independent variable. For instance, analyzing complicated samples may require the whole voltammogram to determine the analyte concentration.[9] Polynomial regression can be also treated similar to the multiple linear regression.[3] For example, the function $y = \beta_0 + \beta_1 x + \beta_2 x^2 + \beta_3 x^3$ can be viewed as the multiple linear regression involving three independent variables. In this case, the linear function can be written in the vectorized form as

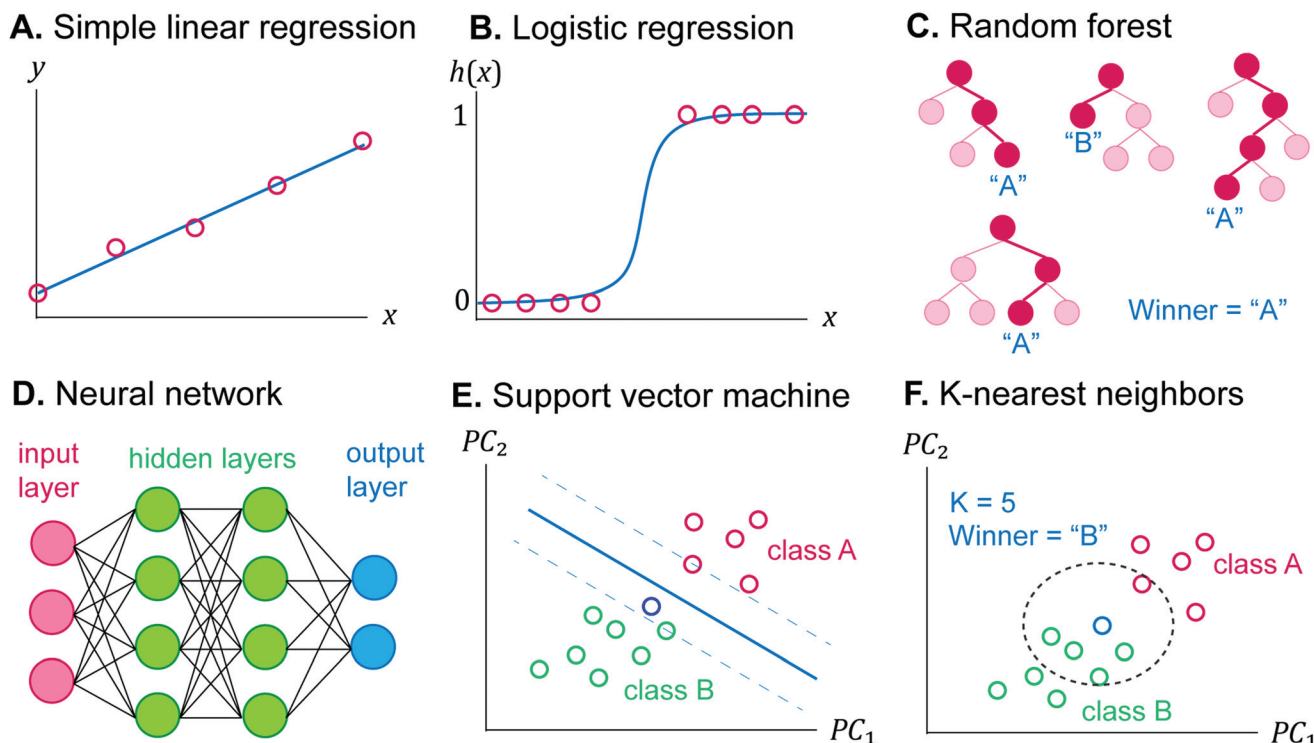$$y = \boldsymbol{\beta}^T \boldsymbol{x} \qquad (3)$$

Fig. 4 Visualization of common machine learning algorithms. (A) Simple linear regression between y and x. (B) Logistic regression with sigmoidal curve mapping x to the probability of being positive $h(x)$. (C) Random forest of four different decision trees votes the data point to be in class A. (D) Neural network with three features in the input layer, two hidden layers, and two nodes in the output layer. (E) Support vector machine with a linear boundary in PC_1–PC_2 spaces. The new blue datapoint falls into class B boundary. (F) K-Nearest neighbors with two groups plotted in PC_1–PC_2 spaces. A dashed line circled $K = 5$ nearest points to the new blue data point being grouped into class B.

where $\boldsymbol{x} = [1 \ x \ x^2 \ x^3]^T$ and $\boldsymbol{\beta} = [\beta_0 \ \beta_1 \ \beta_2 \ \beta_3]^T$. Nevertheless, the mathematics to optimize for the best $\boldsymbol{\beta}$ is the same as that of the simple linear regression.

Logistic regression. There are more ML algorithms for classification problems because the decision rules can be more complicated with their nonlinear nature. For a binary classification ("positive" vs. "negative"), the label of the training set is converted to the numerical 1 for positive and 0 for negative. Logistic regression models the logistic function between the label h and features $\boldsymbol{x}$ as (4).[9,40]

$$h(\boldsymbol{x}) = \frac{1}{1 + \exp\left(-\boldsymbol{\beta}^T \boldsymbol{x}\right)} \tag{4}$$

The graph of $h(\boldsymbol{x})$ resembles the sigmoid curve (Fig. 4B), and the shape allows the binary classification into positive ($h(\boldsymbol{x}) = 1$) or negative ($h(\boldsymbol{x}) = 0$). Notice that the logistic function fitting is done by finding the best $\boldsymbol{\beta}$, similar to (2) or (3). The model can be evaluated on their accuracy by determining $h(\boldsymbol{x})$ of the test set and comparing with their true labels. Logistic regression can also classify more than two classes. Each class has different $h_i(\boldsymbol{x})$, and the class of each training example can be determined from the class giving the highest $h_i(\boldsymbol{x})$.[44]

Decision tree and random forest. Another classification model is the decision tree, which optimizes the decision criteria in each branching point in a tree to classify a data point from its features (Fig. 4C).[42] In each tree, the most effective feature and cutoff is the first branching point, then the training set is sorted through it. The undecided data will be then used to build another branching point until all the samples are correctly identified. Decision tree is one of the most understandable algorithms, but it has high variance, i.e., a slight change of the training set significantly impacts the decision criteria. Random forest improves this limitation by aggregating many trees built from the bootstrapped data subset (Fig. 4C).[9,39] Since each tree is built from a different data subset, there will be hundreds of different trees. Each tree will "vote" by classifying an example with its decision criteria, and the highest vote will be the class of that example.[45] While the nature of random forest is classification, the class can be substituted with the numerical output for the regression problem.[46]

Artificial neural network. One of the most popular ML algorithms to analyze hidden nonlinear relationships is artificial neural network, or neural network, in short.[9,47] Neural networks have been designed by mimicking the interconnection and activation of brain neurons.[9] A typical neural network consists of an input layer, hidden layer(s), and an output layer with the interconnection between the nodes in each layer (Fig. 4D). Specifically, ML using a neural network with mul-

tiple hidden layers is called deep learning.[39] The nodes in the input layer contain the value of each feature, such as current at each applied potential. The values from each node will be combined with different weights, usually by linear combination and followed by the activation function (such as logistic function, hyperbolic tangent, or rectified linear unit) to get the value of the first hidden layer, usually between 0 and 1 to determine the nodes to be activated. The values of the first hidden layer will be combined in the same way with a new set of weights to yield the values of nodes in the next hidden layer. The calculation is repeatedly performed until the output layer. Each node in the output layer shows the probability of the sample being in each class. Therefore, the training task is to optimize the weights in each linear combination to get the highest prediction accuracy from the output layer.[9] There are also many special architectures of neural networks, such as convolutional neural network (CNN)[48] and recurrent neural network[49] that are designed for image analysis and time-series data, respectively.[9] Neural networks are useful for both classification and regression problems, the latter can be done by substituting the activation function in the last activation by a regression function.[50]

Support vector machine. Support vector machine (SVM) classifies data points by finding a hyperplane that best separates the data points from different classes (Fig. 4E).[9] The best hyperplane has the most distance from the data point from each class. While the application is similar to that of logistic regression, SVM can be performed on non-linear boundary decisions by introducing a kernel to add more dimensions to the feature space. SVM gives a definitive "yes" or "no" answer based on the area that the data point falls into, different from logistic regression which gives the continuous probability.[51] Moreover, SVM can be extended to perform regression by adding a tolerance to the regression line to calculate the numerical output, and the algorithm will find the line which best fits to the data with the least amount of data falling out of the tolerance boundary.[52]

***K*-Nearest neighbors.** *K*-Nearest neighbors (KNN) is another ML algorithm for classification.[9,51] Data points with their known label or group are plotted in the feature space or transformed space (such as PCA). When a new data point is fed to the algorithm, it will count the label of the *K* nearest data points (Fig. 4F), and the label with the highest "vote" will be its label. Although the nature of KNN is classification, it can be implemented for regression as well by averaging the label of the nearest data points. Since the algorithm is simple, the appropriate *K*, feature selection, and data transformation must be carefully optimized.[3]

3.3. Machine learning implementation

There are many steps in implementing ML.[39] First, the data are collected, preprocessed, and split into training, cross validation, and test sets. Then, the ML algorithm must be chosen based on the nature of the problem (classification or regression, linear or nonlinear, zero, first, or second-order). Next, the algorithm learns from the training set to find the

best decision rule. In general, coefficients and weights in the first learning iteration are randomized and predict the output of the training set, and the difference between the predicted output and the true output is evaluated as a "cost" or "loss", such as mean squared error as in the simple linear regression. Subsequently, the cost is used to update the coefficients and weights in the right gradient and direction by a method such as gradient descent, and the updated parameters are used in the next iteration. These steps are iterated until the prediction accuracy of the training set is satisfactory.

The selected ML model requires optimization of the architecture as well, such as the highest degree in polynomial regression or the *K* in KNN. These internal parameters are called hyperparameters.[47] Hyperparameters are optimized by evaluating the prediction accuracy of the cross validation set by the models optimized from the training set with different hyperparameters. Finally, the best ML model and architecture are evaluated by the prediction accuracy and other performance parameters with the test set, which can be compared with those of other models to find the best ML algorithm to be implemented in the future.

3.4. Machine learning for the investigation of electrochemistry and electrode materials

Determining electrochemical parameters and mechanisms. ML algorithms have been implemented to determine the thermodynamics, kinetics, and mass transfer properties of electroactive species in electrochemical experiments.[53] Applications of ML for extracting electrochemical parameters can be dated back to 1979, when the KNN model was implemented to determine the heterogeneous electron transfer kinetic parameters of five metal ions from polarography at the dropping mercury electrode.[54] The work uses synthetic polarograms with known parameters as the training set. Fourier transform was also applied to polarograms to eliminate the noise, and several measures of distance to determine the nearest neighbors were compared. This work illustrated that choosing a simple ML model requires the optimization of hyperparameters and data preprocessing. In a recent review, Gundry *et al.* also discussed the applications of Bayesian inference and ML to deduce electrochemical parameters from alternating current voltammetry.[53] This approach alleviates noise and frequency-independent response such as background current and greatly enhances electrochemical information from the frequency-dependent signal. Using ML and automated algorithms can help to reduce human error from choosing a wrong electrochemical model and assumption for simulation and numerical analysis.

Currently, ML algorithms have been implemented to identify the electrode reaction mechanism from electrochemical data, since this step typically needs human decision and is prone to human errors. For example, SVM was utilized to identify the equivalent circuit of the electrode reaction from the EIS Nyquist plots.[45] SVM was trained from the database consisting of over 500 published spectra classified into five circuit models, and it performed better than other models

such as decision tree and random forest. For CV, the Bond group sought an alternative approach to classify the experimental and simulated voltammograms into different electrode reaction mechanisms (E, EE, and EC).[55] Because the CV shape

depends on such mechanisms, the voltammograms were treated as images instead of numerical data, and the problem became image recognition, which was solved by the convolutional neural network (CNN) (Fig. 5A). The algorithm correctly
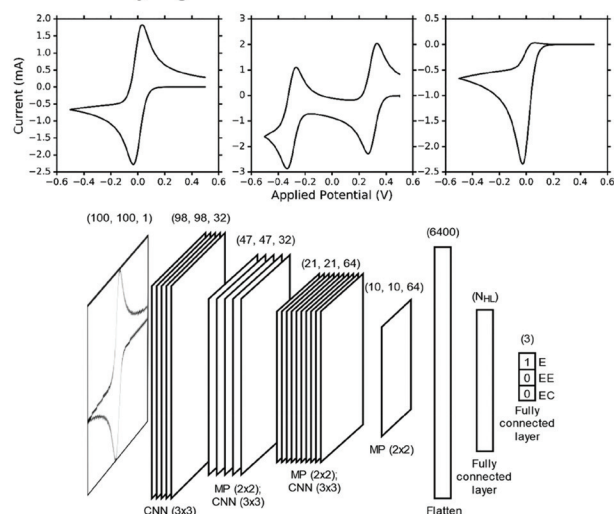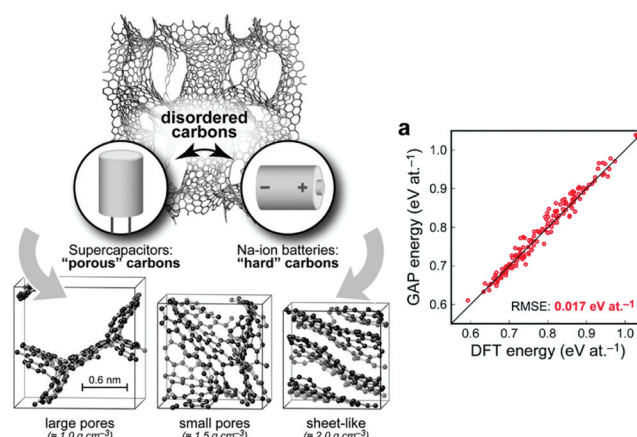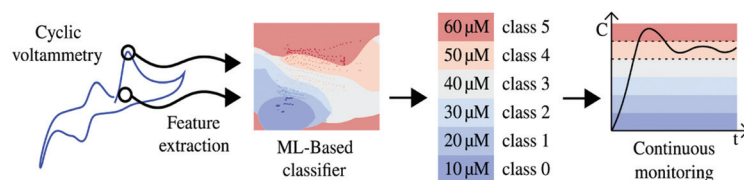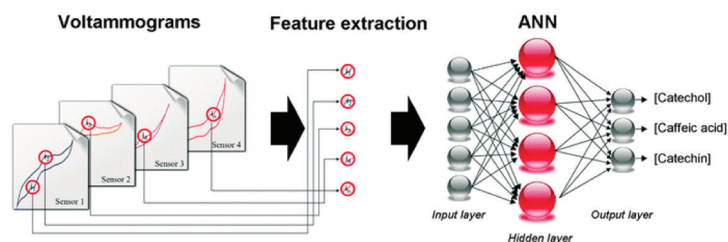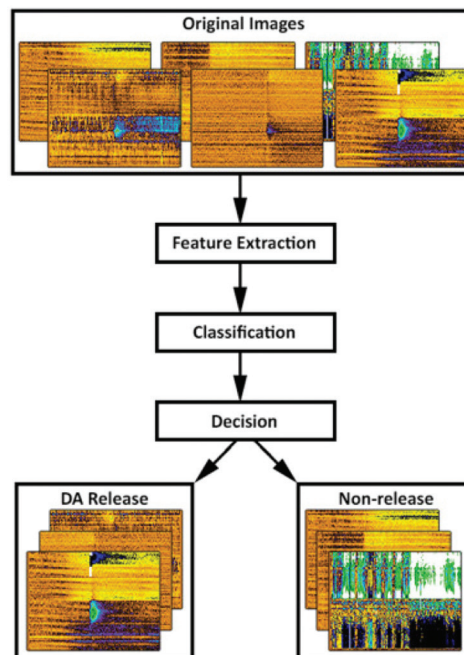

Fig. 5 Examples of machine learning applications for electrochemical sensors. (A) Deep CNN identifies the electrode reaction mechanism from CVs. Adapted with permission from ref. 55. Copyright 2019 American Chemical Society. (B) GAP-based ML predicted the structure of amorphous carbons and their energies. Adapted with permission from ref. 60. Published by The Royal Society of Chemistry. (C) SVM classified the CV of propofol into a level of concentration to aid the continuous monitoring. Adapted from ref. 52 with permission from Elsevier (Copyright 2021). (D) Neural network combined the CVs from electronic tongue to identify and quantify amounts of polyphenolic compounds. Adapted from ref. 62 with permission from The Royal Society of Chemistry. (E) Neural network detects dopamine FSCV from the false color plot. Adapted from ref. 48 with permission from Elsevier (Copyright 2020).

identified the mechanism with 89% accuracy, the misclassification was similar to human's decisions, and the effect of noise, resistance, and scan rate on the accuracy was also extensively studied. Whether these ML models can also determine other electrode reaction parameters directly from the data should be explored in the future.

Optimizing electrode material structure and properties. It is worth mentioning some reports in using ML to optimize an electrode material, which is informative to develop a high-performance electrochemical sensor. Carbon electrodes are popular in developing an electrochemical sensor.[56–58] However, carbon structures are diverse and not straightforward to be controlled in the synthesis since they are sensitive to the experimental condition. Caro *et al.* utilized a neural network based on the Gaussian approximation potential (GAP) to model the interatomic potential of carbon structures for the deposition and growth of amorphous carbon films by recalculating the energy after adding a new carbon atom.[59] This approach revealed that the amorphous carbon growth mechanism depends on the energy of the new carbon atom. In another work, Deringer *et al.* combined DFT and GAP to study the effect of pore size and intercalating atoms on the carbonaceous electrode material for Na-ion batteries and supercapacitors.[60] The model was trained from the DFT data of different structures with their experimental potential, then the atomic potential-energy surface of the modeled carbon structure was predicted (Fig. 5B). In both studies, the accuracy of the ML algorithm was close to that of DFT calculation with the benefit of lower computational cost. Another work by Rohr *et al.* reported a catalyst for the oxygen evolution reaction (OER) by sequential learning, a stepwise ML algorithm that optimizes the ML model based on the performance of the previous model.[61] 2121 metal oxides from 6 metal ions with different compositions and mixtures were high-throughput synthesized, and their OER overpotentials were determined experimentally to build the training set for ML. The sequential learning performance was then compared between using random forest, Gaussian process, and linear ensemble, which was suitable for different tasks. In the future, these strategies could be used to extract knowledge on the structure and electrochemical properties of electrode materials or chemical/biorecognition elements.

3.5. Machine learning for the analysis of signals from electrochemical sensors

Nonlinear calibration. Most electrochemical sensors employ simple linear regression to determine the analyte concentration. However, many phenomena, such as electrode fouling and surface renewing, cause the change in the sensitivity and the deviation from the linearity. To solve this problem, ML has been implemented to extract other electrochemical signals such as peak width and background current to construct a better calibration curve. For example, Aiassa *et al.* used SVM to quantify the concentration of propofol from staircase CV (Fig. 5C).[52] Because propofol undergoes electropolymerization and fouls the electrode, the simple linear regression is not accurate. The propofol peak potential, electron transfer charge, and consecutive run number were included in the SVM model to predict the propofol concentration; the prediction accuracy was improved from 67% to 100% because the SVM model took electrode fouling into account in addition to the propofol signal. In another work, Rivera *et al.* successfully used random forest and neural network to predict the concentration of Ru(bpy)$_3^{2+}$ from electrogenerated chemiluminescence data including maximum current, minimum derivative in the chronoamperogram, and decay slope of the luminescence intensity.[46] SVM was also utilized to analyze EIS spectra to quantify acetone by a chemosensory protein biosensor to enhance the weak signal from the binding between acetone and biological recognition elements.[63] These studies showed that using some but not all information from the voltammogram helps reduce the training computation cost and time while still yielding better performance than the univariate calibration.

There are some studies that utilize neural networks for quantitative analysis. The Wen group trained a neural network by feeding the peak current–concentration pairs as a training set before using the model to predict the unknown concentration from the electrochemical data. This method was used to determine the amount of amaranth at the MWCNT/N-doped graphene/PEDOT:PSS electrode[64] and maleic hydrazide at PEDOT–COOH modified with copper nanoparticles by DPV.[50] In both studies, the nonlinear relationship between the concentration and peak current was obtained, so the prediction accuracy was improved. More condition variations such as pH changes, fouling compounds, or more real samples could be included to test the robustness of the prediction.

Chemical identification. ML is a powerful tool for identifying a chemical species giving complex signals from electrochemical sensors, especially for discriminating similar species giving almost identical signals. For instance, the del Valle group implemented a neural network algorithm with discrete wavelet transformed (DWT) voltammograms to resolve and quantify the concentrations of dopamine, serotonin, ascorbic acid, and uric acid, which have broad faradaic peaks that can overlap and interfere with each other.[65] Using DWT reduced the amount of data for neural network training and prediction while still yielding better performance than classical analysis such as partial least squares (PLS) regression. In another work, ML models were compared to aid the multiplex analysis of heavy metal ions (Cu, Cd, Hg, Pb, Zn, and Ag) by SWV.[66] Forward and backward voltammograms were decomposed from the total voltammogram to emphasize the charging current difference, and the PCA-processed voltammogram with SVM classifier performed superior (over 90% accuracy) to other methods such as decision tree or KNN. Nevertheless, the concentration and pH of the supporting electrolyte in both studies still strongly influenced the accuracy and can be included in the future models.

ML models were also applied to analyze electrochemical signals from cyclic square wave voltammetry (CSWV), which combines selectivity from CV with sensitivity enhancement

from SWV.[49] Dean *et al.* compared the performance of different ML algorithms in classifying heavy metals and explosives in seawater from CSWV analysis.[49] Evaluated by the F_1 score, CNN and long-short term memory (LSTM) performed better than simple dimensionality reduction techniques such as SVM and PCA. While CNN is widely accepted for image recognition problems, it is interesting that LSTM, which is commonly used for time-series data analysis, also exhibited superior performance. Furthermore, the combination of CNN and LSTM also enhanced the classification performance, and it was also used with a multilayer epitaxial graphene electrode for metal ions and pesticide contaminant detection in seawater by the same research group.[67]

Electronic tongue. To improve the limited selectivity from using a single electrode, an electronic tongue or nose has been proposed by mimicking the olfactory system consisting of many receptors. An electrochemical electronic tongue or nose is a set or array of different electrodes giving different responses to a chemical species, and a combination of the signals can help identify a chemical species or geographical information of a product.[68] This allows ML to jump in as an effective strategy to develop and train these electronic tongues.[69] For instance, a voltammetric tongue was constructed from a three-electrode array of graphite-epoxy composite modified with different crown ether hosts for the simultaneous quantification of Cd, Pb, and Hg ions by differential pulse anodic stripping voltammetry.[70] Three voltammograms from these three electrodes were transformed by DWT and analyzed by a neural network of 93 input nodes, a four-neuron hidden layer, and three output nodes representing the concentration of each metal ions. This approach improved the quantification from using simple linear regression with individual crown ether hosts, since each of them may not be perfectly specific to a single metal ion. In another work, Wesoły *et al.* proposed a potentiometric electronic tongue to classify sweeteners in pharmaceutical products from an array of 16 ion-selective electrodes.[51] While SVM provided the best performance from the analysis of steady-state potentiometric responses, other algorithms such as soft independent modelling of class analogies (SIMCA) and PLS improved the analysis of dynamic potentiometric responses which were different because of different binding kinetics between sweeteners and host on the electrodes.

Furthermore, electronic tongues possess the potential to identify the geographical-dependent products and their authenticity. For example, ML was used to identify wine with different polyphenolic compounds from CVs obtained from four enzyme-modified electrodes.[62] DoE feature selection was performed to choose 23 significant potential points from the voltammogram for neural network regression with three output nodes, corresponding to the amount of three polyphenolic antioxidants giving the electrochemical signals (Fig. 5D). Wang *et al.* also developed nanocomposite-modified glassy carbon electrodes to distinguish Chinese rice wines from different geographical origins by a deep learning algorithm trained from 200 PCA-transformed CV and SWV,[71] where the electrochemical signal was produced from electroactive components including 5′-GMP, Tyr, and GA in the rice wines. While the classification accuracy was over 95%, the neural network needed 50 hidden layers, which may require a long training duration.

Temporal information from electrochemical measurements can also provide better differentiation for electronic tongues. Analyzing temporal patterns require a time-series algorithm, and automation is essential for continuous measurement such as in environmental or wearable sensors. For example, an electronic nose for malodor detection was constructed from ten commercial electrochemical gas sensors for H_2S, NH_3, and SO_2 detection.[72] The smoothed temporal responses with their features (amplitude, average, and variance) were trained by different learning models to distinguish odor. Different ML models were suitable for different tasks, *e.g.*, to determine whether the odor is offensive or to differentiate offensive odors. The same scheme of time-series analysis could be applied in other continuous measurements such as pollution control or smart home devices.

Second-order data. Second-order electrochemical data reveal electrochemical fingerprints from complement properties such as temporal or spectroscopic properties. FSCV has been utilized in neurochemistry for the real-time monitoring of neurotransmitters *in vivo*.[37,73] Traditionally, FSCV gives the false color plot of current–potential–time data, which allows researchers to identify the neurotransmitter from colors and their shapes and positions from the image-like data. However, many neurotransmitters have the same electroactive moiety and thus give virtually the same shape, so manual identification by humans is difficult and could be automated by ML. Zhang *et al.* designed a deep neural network to determine the dopamine concentration from FSCV voltammograms.[74] The training set was built from the *in vitro* FSCV of dopamine with five different concentrations and five electrodes, then it was used to train a 10-layer neural network with 850 input nodes representing current at each potential point and two output nodes for the electrode and concentration. The authors also proposed the data compression strategy to reduce the computational cost so that the algorithm can be implemented in a wearable FSCV device without the loss of performance. Alternatively, Matsushita *et al.* utilized the pre-designed neural network to distinguish dopamine FSCV (Fig. 5F).[48] By considering the false color plots as images, a successful CNN YOLOv3 was implemented to achieve over 96% accuracy in the identification of dopamine signals *in vivo*. Future improvement could be to extend to analyze other neurotransmitters and provide fast and real-time identification.

Nevertheless, CNN could be applied to other electrochemical techniques giving second-order data, such as three-dimensional or multiple step chronoamperometry. This technique applies a series of different potentials to collect a set of chronoamperograms to obtain the electrochemical properties of different electroactive species.[75] Previously, classical methods such as parallel factor analysis and multivariate curve resolution alternating least squares were applied to such data

to differentiate the electrochemical signal from similar compounds.[76] ML indeed has the potential to improve the analysis of the three-dimensional surface obtained from the technique.

4. Moving forward to the future of electrochemical sensors and biosensors by machine learning and experimental design

4.1. Reducing chemicals, time, and waste in developing electrochemical sensors

One of the major goals of DoE is to reduce the number of optimizing experiments by strategically choosing the values of independent variables to test.[17] Decreasing the number of experiments also decreases the chemical and reagent usages, improves the working efficiency, and reduces the generated waste from the experiment. Therefore, implementing DoE in developing sensors meets the scope of green chemistry, which investigates the practice of carefully designed chemical processes to improve their efficiency and sustainability.[77] Although systematic DoEs have been available for many decades, they were not widely adapted to optimize electrochemical sensors, with the OFAT approach still dominating the field. OFAT, however, is not useless—it should be used when studying or discovering new materials or systems. When obtaining their capabilities, the systematic DoE should be then performed to optimize the sensor fabrication. ML can also be a useful tool to find the appropriate chemical structure and composition for the best electrochemical sensor.

As DoE should be a common method to optimize any system, including DoE in sensor research should not be the focus of the work *per se*. Emphasizing DoE without regarding the chemical aspect of the work blurs the actual novelty and discourages the discussion on how the sensor component improves its analytical performance. Instead, DoE should be a tool for understanding the effect of each sensor component, detection condition, and their synergistic effects. DoE indeed will be an important tool to develop point-of-care diagnostics while achieving the goal of green chemistry and sustainability simultaneously.

4.2. Pushing the analytical performance of electrochemical sensors

An ideal electrochemical sensor must possess high selectivity, high sensitivity, and low LoD, as well as high reproducibility and repeatability. The traditional, chemical approach to improve a sensor to meet those criteria is to increase the signal-to-noise ratio by fabricating electrocatalytic materials, conducting polymers, and selective recognition elements on the sensor.[78,79] Ratiometric sensors have been also proposed to correct the sensitivity being altered from the baseline change.[80] ML and DoE are useful to investigate and optimize the best sensor composition. However, with the availability of signal processing tools such as Fourier transform and digital filters, these methods have been successfully complemented to the chemical approach to improve the sensor.[38,81,82] Accordingly, the question now is how signal processing and analysis by ML can improve the figures of merit of electrochemical sensors. Recently, Cho *et al.* implemented ML to detect H_2 below the chemical LoD using a metal resistive gas sensor.[83] With a deep neural network structure for anomaly detection, H_2 with ultralow concentration (<10 ppm) can be detected from the temporal resistivity profile. Furthermore, more theoretical work could be done to formalize how to evaluate the quantitative parameters such as sensitivity and LoD for ML regression, as in the work by Chiappini *et al.*, suggesting to estimate the sensitivity of the neural network from the uncertainty of the output and input.[84] Being able to quantify the figures of merit with low LoD will accelerate applications of electrochemical sensors where the clinically relevant concentration is extremely low, such as SARS-CoV-2 diagnosis.[85]

4.3. Validating electrochemical sensors for point-of-care diagnostics and commercialization

Novel biosensors for point-of-care diagnostics are currently being treated as devices for screening purposes only. Their reliability issues from the performance-portability tradeoff impede them from making the final decision. Commercialized and wearable sensors are also subjected to similar problems as they are affected by varied temperature and noise.[86] ML can help the developed sensors to overcome this agenda by learning the fingerprint of the chemicals and biomarkers from a wide range of training sets and experimental conditions.[87] This objective has been accomplished in nonspecific detection such as artificial nose and tongue that realize for a group of similar chemical species. For instance, Kim *et al.* reported a surface-enhanced Raman scattering nose from a nanostructured gold surface modified with different surface functional groups (amine, hydroxyl, carboxyl, and methyl) to distinguish lipid, nucleic acid, and proteins by linear discriminant analysis.[88] Thus, combining the selectivity from ML and recognition elements of the electrochemical sensor will greatly enhance the reliability and will push the application for the real settings.

One key important issue is the limited heterogeneity of the database to train the ML algorithm. ML generally performs well with the data similar to or generated from the same environment as the training set, but testing it with the data from a new system or country frequently results in the failure.[89] Training the ML algorithms with a wide range of possible detection conditions will help it recognize the pattern and chemical fingerprint, which will improve the performance and reliability of electrochemical sensors. This task requires an expansive database of electrochemical data to train and test the ML algorithm. In the foreseen future, automated robot experimenters might be invented and used to generate exhaustive data to save human time and energy.[90] Another concern regarding electrochemical data is their sensitivity to the instru-

mentation, thus their identity might need to be included. Nevertheless, compared to other gold-standard methods, electrochemical sensors are truly portable and can be affordable and efficient household devices. Accordingly, ML will be a crucial key for point-of-care diagnostics devices and commercialized sensors for biomedical, food, and environmental monitoring with reliable results.

4.4. Training chemists to approach the future

There are two approaches to encourage the applications of ML and DoE in electrochemical sensors. One approach is that chemists can collaborate with outside experts or statisticians to initiate the project and solve the problem when applying these unfamiliar methods in their analytical chemistry work. Without conceptual understanding, chemists may treat these ML and DoE methods as a black box, preventing them from choosing and optimizing the algorithm, while those experts may not understand the chemical problems that chemists try to solve. Another approach that is more sustainable is to train current and future chemists on DoE and ML. Traditionally, chemistry students may be required to take a course in statistics, but it is apparently inadequate for today and tomorrow. A course or short training on DoE, programming, and ML will be useful for the future chemists to understand the nature of these tools and appropriately apply them in their research. Combining these tools with chemical insights will enhance their creativity to propose novel solutions for significant scientific problems, including how to make a better electrochemical sensor to improve quality of life.

5. Conclusions

In this article, we summarize and discuss the progress and thoughts in DoE and ML applications to optimize electrochemical sensors and to analyze complicated electrochemical data that are emerging and turning the field of analytical chemistry. Choosing appropriate DoE instead of the OFAT design enables simultaneous optimization of parameters related to electrode fabrication. DoE also considers interactions between factors, while saving the time and cost from non-essential experiments, and RSM is a useful methodology to optimize such effects on the response to aid the optimization of the electrochemical sensor. To investigate how electrode chemical structures affect their electrochemical properties, ML has proved itself to be a versatile tool for both regression and classification. Utilizing ML algorithms such as a neural network and SVM is superior to analyze potentiometric, voltammetric, and impedimetric data from electrochemical sensors and electronic tongues, as they are advantageous over classical univariate methods. The successful implementation of DoE and ML will contribute to chemical sustainability, enhance the sensor performance, and accelerate the applications of complex electrochemical sensors in the broadest sense.

Conflicts of interest

There is no conflict of interest to declare.

Acknowledgements

References

1 C. Zhu, G. Yang, H. Li, D. Du and Y. Lin, *Anal. Chem.*, 2015, **87**, 230–249.

2 A. Suea-Ngam, L. Bezinge, B. Mateescu, P. D. Howes, A. J. DeMello and D. A. Richards, *ACS Sens.*, 2020, **5**, 2701–2723.

3 M. D. Peris-Díaz and A. Krężel, *TrAC, Trends Anal. Chem.*, 2021, **135**, 116157.

4 S. Tortorella and S. Cinti, *Anal. Chem.*, 2021, **93**, 2713–2722.

5 M. I. Jordan and T. M. Mitchell, *Science*, 2015, **349**, 255–260.

6 W. P. Walters and R. Barzilay, *Acc. Chem. Res.*, 2021, **54**, 263–270.

7 S. Namuduri, B. N. Narayanan, V. S. P. Davuluru, L. Burton and S. Bhansali, *J. Electrochem. Soc.*, 2020, **167**, 037552.

8 M. Mayer and A. J. Baeumner, *Chem. Rev.*, 2019, **119**, 7996–8027.

9 L. B. Ayres, F. J. V. Gomez, J. R. Linton, M. F. Silva and C. D. Garcia, *Anal. Chim. Acta*, 2021, **1161**, 338403.

10 A. Isozaki, J. Harmon, Y. Zhou, S. Li, Y. Nakagawa, M. Hayashi, H. Mikami, C. Lei and K. Goda, *Lab Chip*, 2020, **20**, 3074–3090.

11 A. Suea-Ngam, P. D. Howes, M. Srisa-Art and A. J. DeMello, *Chem. Commun.*, 2019, **55**, 9895–9903.

12 Y. Zhang, Q. Tang, Y. Zhang, J. Wang, U. Stimming and A. A. Lee, *Nat. Commun.*, 2020, **11**, 6–11.

13 O. Allam, R. Kuramshin, Z. Stoichev, B. W. Cho, S. W. Lee and S. S. Jang, *Mater. Today Energy*, 2020, **17**, 100482.

14 Y. Chen, B. Tian, Z. Cheng, X. Li, M. Huang, Y. Sun, S. Liu, X. Cheng, S. Li and M. Ding, *Angew. Chem.*, 2021, **60**, 4199–4207.

15 R. Mahbub, K. Huang, Z. Jensen, Z. D. Hood, J. L. M. Rupp and E. A. Olivetti, *Electrochem. Commun.*, 2020, **121**, 106860.

16 L. Wilbraham, S. H. M. Mehr and L. Cronin, *Acc. Chem. Res.*, 2021, **54**, 253–262.

17 R. G. Brereton, *Applied Chemometrics for Scientists*, John Wiley & Sons, Ltd, Chichester, UK, 2007.

18 A. V. Filgueiras, J. Gago, I. García, V. M. León and L. Viñas, *Mar. Pollut. Bull.*, 2021, **162**, 111841.

19 J. D. Kechagias, K.-E. Aslani, N. A. Fountas, N. M. Vaxevanidis and D. E. Manolakos, *Measurement*, 2020, **151**, 107213.

20 K. Chindaphan, K. Wongravee, T. Nhujak, T. Dissayabutra and M. Srisa-Art, *J. Sep. Sci.*, 2019, **42**, 2867–2874.

21 S. Wirojsaengthong, D. Aryuwananon, W. Aeungmaitrepirom, B. Pulpoka and T. Tuntulani, *Talanta*, 2021, **231**, 122371.

22 C. García-Gómez, P. Drogui, F. Zaviska, B. Seyhi, P. Gortáres-Moroyoqui, G. Buelna, C. Neira-Sáenz, M. Estrada-alvarado and R. G. Ulloa-Mercado, *J. Electroanal. Chem.*, 2014, **732**, 1–10.

23 M. Ahmadi and F. Ghanbari, *Environ. Sci. Pollut. Res.*, 2016, **23**, 19350–19361.

24 M. A. Bezerra, R. E. Santelli, E. P. Oliveira, L. S. Villar and L. A. Escaleira, *Talanta*, 2008, **76**, 965–977.

25 A. Suea-Ngam, P. Rattanarat, K. Wongravee, O. Chailapakul and M. Srisa-Art, *Talanta*, 2016, **158**, 134–141.

26 A. Suea-Ngam, P. D. Howes, C. E. Stanley and A. J. DeMello, *ACS Sens.*, 2019, **4**, 1560–1568.

27 A. Suea-Ngam, L.-T. Deck, P. D. Howes and A. J. DeMello, *Anal. Chim. Acta*, 2020, **1135**, 29–37.

28 T. Ören Varol, B. Perk, O. Avci, O. Akpolat, Ö. Hakli, C. Xue, Q. Li and Ü. Anik, *Measurement*, 2019, **147**, 14–19.

29 B. Brahma, S. Sen, P. Sarkar and U. Sarkar, *Anal. Chim. Acta*, 2021, **1168**, 338595.

30 H. A. M. Hendawy, A. M. Ibrahim, W. S. Hassan, A. Shalaby and H. M. El-sayed, *Microchem. J.*, 2019, **145**, 428–434.

31 J. L. da Silva, E. Buffon, M. A. Beluomini, L. A. Pradela-Filho, D. A. Gouveia Araújo, A. L. Santos, R. M. Takeuchi and N. R. Stradiotto, *Anal. Chim. Acta*, 2021, **1143**, 53–64.

32 K. S. Rizi, B. Hatamluyi, M. Rezayi, Z. Meshkat, M. Sankian, K. Ghazvini, H. Farsiani and E. Aryan, *Talanta*, 2021, **226**, 122099.

33 J. M. Díaz-Cruz, M. Esteban and C. Ariño, *Chemometrics in Electroanalysis*, Springer International Publishing, Cham, 2019.

34 E. Zdrachek and E. Bakker, *Anal. Chem.*, 2021, **93**, 72–102.

35 G. Moro, H. Barich, K. Driesen, N. Felipe Montiel, L. Neven, C. Domingues Mendonça, S. Thiruvottriyur Shanmugam, E. Daems and K. De Wael, *Anal. Bioanal. Chem.*, 2020, **412**, 5955–5968.

36 J. J. A. Lozeman, P. Führer, W. Olthuis and M. Odijk, *Analyst*, 2020, **145**, 2482–2509.

37 P. Puthongkham and B. J. Venton, *Analyst*, 2020, **145**, 1087–1102.

38 P. Puthongkham, J. Rocha, J. R. Borgus, M. Ganesana, Y. Wang, Y. Chang, A. Gahlmann and B. J. Venton, *Anal. Chem.*, 2020, **92**, 10485–10494.

39 F. Cui, Y. Yue, Y. Zhang, Z. Zhang and H. S. Zhou, *ACS Sens.*, 2020, **5**, 3346–3364.

40 T. Hastie, R. Tibshirani and J. Friedman, *The Elements of Statistical Learning*, Springer New York, New York, NY, 2009.

41 M. Tuck, L. Blanc, R. Touti, N. H. Patterson, S. Van Nuffel, S. Villette, J. C. Taveau, A. Römpp, A. Brunelle, S. Lecomte and N. Desbenoit, *Anal. Chem.*, 2021, **93**, 445–477.

42 K. P. Murphy, *Machine Learning: A Probabilistic Perspective*, The MIT Press, 2012.

43 R. B. Keithley, R. Mark Wightman and M. L. Heien, *TrAC, Trends Anal. Chem.*, 2009, **28**, 1127–1136.

44 A. Barati Farimani, M. Heiranian and N. R. Aluru, *npj 2D Mater. Appl.*, 2018, **2**, 14.

45 S. Zhu, X. Sun, X. Gao, J. Wang, N. Zhao and J. Sha, *J. Electroanal. Chem.*, 2019, **855**, 113627.

46 E. C. Rivera, J. J. Swerdlow, R. L. Summerscales, P. P. T. Uppala, R. M. Filho, M. R. C. Neto and H. J. Kwon, *Sensors*, 2020, **20**, 625.

47 K. T. Butler, D. W. Davies, H. Cartwright, O. Isayev and A. Walsh, *Nature*, 2018, **559**, 547–555.

48 G. H. G. Matsushita, A. H. Sugi, Y. M. G. Costa, A. Gomez-A, C. Da Cunha and L. S. Oliveira, *Comput. Biol. Med.*, 2019, **114**, 103466.

49 S. N. Dean, L. C. Shriver-Lake, D. A. Stenger, J. S. Erickson, J. P. Golden and S. A. Trammell, *Sensors*, 2019, **19**, 2392.

50 Y. Sheng, W. Qian, J. Huang, B. Wu, J. Yang, T. Xue, Y. Ge and Y. Wen, *Microchim. Acta*, 2019, **186**, 543.

51 M. Wesoły and P. Ciosek-Skibińska, *Sens. Actuators, B*, 2018, **267**, 570–580.

52 S. Aiassa, I. Ny Hanitra, G. Sandri, T. Totu, F. Grassi, F. Criscuolo, G. De Micheli, S. Carrara and D. Demarchi, *Biosens. Bioelectron.*, 2021, **171**, 112666.

53 L. Gundry, S. X. Guo, G. Kennedy, J. Keith, M. Robinson, D. Gavaghan, A. M. Bond and J. Zhang, *Chem. Commun.*, 2021, **57**, 1855–1870.

54 R. A. DePalma and S. P. Perone, *Anal. Chem.*, 1979, **51**, 829–832.

55 G. F. Kennedy, J. Zhang and A. M. Bond, *Anal. Chem.*, 2019, **91**, 12220–12227.

56 Q. Cao, P. Puthongkham and B. J. Venton, *Anal. Methods*, 2019, **11**, 247–261.

57 P. Puthongkham and B. J. Venton, *ACS Sens.*, 2019, **4**, 2403–2411.

58 P. Puthongkham, C. Yang and B. J. Venton, *Electroanalysis*, 2018, **30**, 1073–1081.

59 M. A. Caro, G. Csányi, T. Laurila and V. L. Deringer, *Phys. Rev. B*, 2020, **102**, 174201.

60 V. L. Deringer, C. Merlet, Y. Hu, T. H. Lee, J. A. Kattirtzi, O. Pecher, G. Csányi, S. R. Elliott and C. P. Grey, *Chem. Commun.*, 2018, **54**, 5988–5991.

61 B. Rohr, H. S. Stein, D. Guevarra, Y. Wang, J. A. Haber, M. Aykol, S. K. Suram and J. M. Gregoire, *Chem. Sci.*, 2020, **11**, 2696–2706.

62 X. Cetó, F. Céspedes, M. I. Pividori, J. M. Gutiérrez and M. Del Valle, *Analyst*, 2012, **137**, 349–356.

63 Y. Rong, A. V. Padron, K. J. Hagerty, N. Nelson, S. Chi, N. O. Keyhani, J. Katz, S. P. A. Datta, C. Gomes and E. S. McLamore, *Analyst*, 2018, **143**, 2066–2075.

64 T. Xue, P. Liu, J. Zhang, J. Xu, G. Zhang, P. Zhou, Y. Li, Y. Zhu, X. Lu and Y. Wen, *ACS Omega*, 2020, **5**, 28452–28462.

65 M. Bonet-San-Emeterio, A. González-Calabuig and M. del Valle, *Electroanalysis*, 2019, **31**, 390–397.

66 J. J. Ye, C. H. Lin and X. J. Huang, *J. Electroanal. Chem.*, 2020, **872**, 113934.

67 L. C. Shriver-Lake, R. L. Myers-Ward, S. N. Dean, J. S. Erickson, D. A. Stenger and S. A. Trammell, *Sensors*, 2020, **20**, 1–9.

68 E. A. Baldwin, J. Bai, A. Plotto and S. Dea, *Sensors*, 2011, **11**, 4744–4766.

69 W. Hu, L. Wan, Y. Jian, C. Ren, K. Jin, X. Su, X. Bai, H. Haick, M. Yao and W. Wu, *Adv. Mater. Technol.*, 2019, **4**, 1–38.

70 A. González-Calabuig, D. Guerrero, N. Serrano and M. del Valle, *Electroanalysis*, 2016, **28**, 663–670.

71 J. Wang, L. Zhu, W. Zhang and Z. Wei, *Anal. Chim. Acta*, 2019, **1050**, 60–70.

72 J. Zhou, C. M. Welling, M. M. Vasquez, S. Grego and K. Chakrabarty, *IEEE Trans. Biomed. Circuits Syst.*, 2020, **14**, 705–714.

73 B. J. Venton and Q. Cao, *Analyst*, 2020, **145**, 1158–1168.

74 Z. Zhang and A. Z. Kouzani, *Neural Comput. Appl.*, 2021, DOI: 10.1007/s00521-021-06113-4.

75 N. Papadopoulos, C. Hasiotis, G. Kokkinidis and G. Papanastasiou, *Electroanalysis*, 1993, **5**, 99–102.

76 S. G. Lemos and J. Gonzalez-Rodriguez, *Anal. Chim. Acta*, 2020, **1132**, 36–46.

77 P. Anastas and N. Eghbali, *Chem. Soc. Rev.*, 2010, **39**, 301–312.

78 M. M. Barsan, M. E. Ghica and C. M. A. Brett, *Anal. Chim. Acta*, 2015, **881**, 1–23.

79 R. Pilolli, L. Monaci and A. Visconti, *TrAC, Trends Anal. Chem.*, 2013, **47**, 12–26.

80 J. Zhou, L. Zhang and Y. Tian, *Anal. Chem.*, 2016, **88**, 2113–2118.

81 S. Balaji Ramachandran and K. D. Gillis, *J. Neurosci. Methods*, 2018, **293**, 338–346.

82 M. Kang, E. Kim, S. Chen, W. E. Bentley, D. L. Kelly and G. F. Payne, *Biosens. Bioelectron.*, 2018, **112**, 127–135.

83 S. Y. Cho, Y. Lee, S. Lee, H. Kang, J. Kim, J. Choi, J. Ryu, H. Joo, H. T. Jung and J. Kim, *Anal. Chem.*, 2020, **92**, 6529–6537.

84 F. A. Chiappini, F. Allegrini, H. C. Goicoechea and A. C. Olivieri, *Anal. Chem.*, 2020, **92**, 12265–12272.

85 B. D. Kevadiya, J. Machhi, J. Herskovitz, M. D. Oleynikov, W. R. Blomberg, N. Bajwa, D. Soni, S. Das, M. Hasan, M. Patel, A. M. Senan, S. Gorantla, J. E. McMillan, B. Edagwa, R. Eisenberg, C. B. Gurumurthy, S. P. M. Reid, C. Punyadeera, L. Chang and H. E. Gendelman, *Nat. Mater.*, 2021, **20**, 593–605.

86 N. Promphet, S. Ummartyotin, W. Ngeontae, P. Puthongkham and N. Rodthongkum, *Anal. Chim. Acta*, 2021, **1179**, 338643.

87 N. Artrith, K. T. Butler, F.-X. Coudert, S. Han, O. Isayev, A. Jain and A. Walsh, *Nat. Chem.*, 2021, **13**, 505–508.

88 N. Kim, M. R. Thomas, M. S. Bergholt, I. J. Pence, H. Seong, P. Charchar, N. Todorova, A. Nagelkerke, A. Belessiotis-Richards, D. J. Payne, A. Gelmi, I. Yarovsky and M. M. Stevens, *Nat. Commun.*, 2020, **11**, 207.

89 M. Roberts, D. Driggs, M. Thorpe, J. Gilbey, M. Yeung, S. Ursprung, A. I. Aviles-Rivero, C. Etmann, C. McCague, L. Beer, J. R. Weir-McCall, Z. Teng, E. Gkrania-Klotsas, J. H. F. Rudd, E. Sala and C.-B. Schönlieb, *Nat. Mach. Intell.*, 2021, **3**, 199–217.

90 Y. Shi, P. L. Prieto, T. Zepel, S. Grunert and J. E. Hein, *Acc. Chem. Res.*, 2021, **54**, 546–555.